Crocin I delays cellular senescence potentially via modulating SIRT1/PKM2 expression to improve lactate homeostasis *in vitro*

YICHENG FU[1], ZHIWEI DING[2], YUNCHUANG CHANG[2], CHUNXIA WU[1], SANYING WANG[2], GENXIANG MAO[1,2] and HUILI SU[3]

[1]College of Life Science, Zhejiang Chinese Medical University, Hangzhou, Zhejiang 310053, P.R. China; [2]Zhejiang Key Laboratory of Geriatrics, Geriatrics Institute of Zhejiang Province, Zhejiang Hospital, Hangzhou, Zhejiang 310030, P.R. China; [3]Department of Pharmacy, Zhejiang Hospital, Hangzhou, Zhejiang 310030, P.R. China

Received December 22, 2025; Accepted July 3, 2026

DOI: 10.3892/etm.2026.13252

Abstract. Crocin I has a protective effect against D-galactose-induced aging in rat models; however, its specific mechanism on delaying cellular senescence remains unclear. The aim of the present study was to investigate the interventional effect and related molecular mechanism of Crocin I on replicative senescence and premature senescence of human embryonic lung diploid fibroblasts (WI-38) cells. Replicative senescence model was established through long-term culture and passaging to >55 PD. The premature senescence model was established using WI-38 cells treated with 2,2'-azobis-2-methy-propanimidamide dihydrochloride. The cell viability was detected by using a cell counting kit-8 assay, and the effects of Crocin I on senescent phenotype of WI-38 cells were detected by senescence-associated β-galactosidase (SA-β-Gal) staining. In addition, the intracellular reactive oxygen species (ROS) level was detected by flow cytometry, and gene expression levels were detected by quantitative PCR. RNA sequencing analysis was performed to explore the alteration genes in senescent cells and the Crocin I intervention group. The proteins PKM2, SIRT1, p53 and p21 in WI-38 cells were detected by western blotting, whereas cellular lactate level was detected by L-lactic acid content detection kit and pyruvate kinase (PK) enzyme activity was measured using PK activity assay kit. Crocin I promoted cell proliferation within the range of 10-40 μM. In addition, Crocin I decreased the SA-β-Gal staining positive rate on both replicative and premature senescent WI-38 cells. Furthermore, the intracellular ROS level was decreased by Crocin I intervention. The differentially expressed genes were mainly enriched in phosphorylation, oxidation-reduction process, glucose metabolic process, cellular senescence pathway, glycolysis, hippo signaling pathway and pyruvate metabolism. RNA sequencing analysis and molecular docking revealed that PKM2 was one of the potential targets in Crocin I against senescence activity. Furthermore, Crocin I could enhance the expression of SIRT1 following with decreasing the level of PKM2, p21 and p53. Meanwhile, Crocin I significantly decreased the cellular lactate level in WI-38. In conclusion, Crocin I alleviated the replicative and premature senescence of WI-38 cells partially through regulating SIRT1 and PKM2 expression. Furthermore, this function may involve in glycolysis pathway.

Correspondence to: Dr Genxiang Mao, Zhejiang Key Laboratory of Geriatrics, Geriatrics Institute of Zhejiang Province, Zhejiang Hospital, 1,229 Gudun Road, Xihu, Hangzhou, Zhejiang 310030, P.R. China
E-mail: maogenxiang@163.com

Dr Huili Su, Department of Pharmacy, Zhejiang Hospital, 1,229 Gudun Road, Xihu, Hangzhou, Zhejiang 310030, P.R. China
E-mail: huili_su@163.com

Key words: crocin I, cell senescence, SIRT1, PKM2, glycolysis

Introduction

Cellular senescence was initially hypothesized to be caused by the limited proliferative capacity of cells and the arrest of the cell cycle. The arrest of the cell cycle is irreversible and triggers various phenotypic changes, such as the production of an active secretory group, known as the senescence-associated secretory phenotype (SASP) (1). A study had listed 14 hallmarks of aging (2), and among them, cellular senescence was the foundation during the aging biological process. In addition, mitochondrial dysfunction is an important factor leading to cellular aging (3) and the metabolic patterns of abnormal mitochondria differ notably from those of normal mitochondria (4). Following with the global trend of population aging, the larger aging population has resulted in notable issues and become a burden to the society. Therefore, delaying aging and preventing aging related diseases has been a topic of long-term research among humans.

Traditional Chinese medicine (TCM) has a history of use in treating diseases and improving health among the elderly. The TCM system focuses on the human body as a whole and the connections between its various organ systems (5). TCM and therapies (such as acupuncture) are characterized by their wide range of therapeutic effects and demonstrate unique advantages in treating complex diseases (6). For instance, resveratrol, a non-flavonoid polyphenol initially isolated from *Veratrum album*, has been confirmed to potentially

delay aging and improve cell senescence (7). Saffron, another well-known herbal medicine of TCM, is derived from the dried stigmas of *Crocus sativus L* (8). Saffron also has a history of use as a 'food medicine' and dietary supplement to improve life span (9). For example, in addition to regulating menstrual cycles and tranquilizing the mind, saffron also serves as a functional ingredient in gastronomy and herbal tea. Crocin I (the structure displayed in Fig. 1A), a notable active component of saffron (10), has shown to have good therapeutic effects on various central nervous system diseases such as neurodegenerative diseases, mental disorders, epilepsy, convulsions and insomnia, as well as various cardiovascular diseases such as hypertension, hyperlipidemia and atherosclerosis (11). A previous study also showed that Crocin-enriched tomato extracts exert pleiotropic physiological effects in *Drosophila melanogaster*, modulating development, lifespan, locomotor activity, transcriptomic profiles and mitochondrial function. Notably, Crocin prevented the mitochondrial decay caused by H_2O_2 which showed the protective senescence effect against oxidative stress of Crocin in a human glioblastoma cell line (12O150) (12). In addition, Crocin protected SHSY5Y cells against D-galactose (D-gal) induced aging probably through the reduction of intracellular reactive oxygen species (ROS) and advanced glycation end-products (AGEs) formation (13).

Our previous study demonstrated that saffron showed protective effect against D-gal-induced aging in a rat model (14). However, the direct evidence of Crocin regarding its efficacy on cellular senescence and underlying mechanisms are not yet well understood. Thus, the present study aimed to investigate the specific mechanisms on delaying cellular senescence induced by Crocin I. A well-accepted cellular senescence model, human embryonic lung diploid fibroblast (WI-38), was used to investigate the effect of Crocin I on both of the replicative senescence and premature senescence. The premature senescence model was induced by 2,2'-azobis-2-methy-propanimidamide dihydrochloride (AAPH). In addition, RNA-sequencing analysis was performed to explore the potential molecular mechanisms regarding its effect on modulating cellular senescence.

Materials and methods

Reagents. Crocin I (cat no. ST02900120) and Shikonin (cat no. ST78490220) were purchased from Shanghai Standard Biotech Co., Ltd. Dulbecco's modified Eagle's medium (DMEM; cat no. 11965092), Ham's F-12 medium (F12; cat no. 11765054), fetal bovine serum (FBS; cat no. 16140071) and trypsin (cat no. 25200072) were provided by the Invitrogen (Thermo Fisher Scientific, Inc.). The primary antibodies for SIRT1 and $p21^{Waf1}$ (cat no. 2310S; 64016S) were from Cell Signaling Technology Company, Inc. The primary antibodies for p53 and GAPDH (cat no. SC-126; SC-32233) were purchased from the Santa Cruz Biotechnology, Inc. The primary antibody for PKM2 (cat no. HA723370) was purchased from HUABIO. Kits for the cell counting kit (CCK)-8 assay and senescence associated β-galactosidase (SA-β-Gal) staining (cat nos. C0037 and C0602) were purchased from Beyotime Biotechnology. The QIAamp DNA Mini Kit (cat no. 51304) was purchased from Qiagen GmbH. AAPH (cat no. 440914) was purchased from the MilliporeSigma. The L-lactic acid (L-LA) content detection kit and the pyruvate kinase (PK) activity assay kit (cat nos. BC2235 and BC0545) was purchased from Beijing Solarbio Science & Technology Co., Ltd. Sirtinol (cat no. 410536-97-9) was purchased from TargetMol. Super ECL Detection Reagent (cat no. 36208ES60) was purchased from Shanghai Yeasen Biotechnology Co., Ltd.

Cell culture. WI-38 cells were obtained from the American Type Culture Collection (cat. no. VR-977). WI-38 cells are a widely recognized cell model to explore cell senescence (15). WI-38 cells were cultured in DMEM-high glucose medium containing 10% FBS under standard culture conditions of 5% CO_2, 37˚C. When the cells reached 80-90% confluence they were passaged at a ratio of 1:2 or 1:4. The cells were counted before and after passage, and the cell adherence rate (R) was calculated by sampling and counting the cells 20 h after passage. The cumulative population doubling was calculated as $\sum\log_2(D/D_0)$, where D and D_0 are the cell densities at harvest and inoculation, respectively. It is generally considered that cells up to PD30 are young cells; cells with ≥PD55 are replicative senescent cells (16). When the cells reached 80-90% confluence, they were treated with 5 μM shikonin for 24 h to inhibit PKM2 enzyme activity. The cells were pretreated with Sirtinol for 4 h, followed by addition of Crocin I or untreated medium for 24 h. To enhance the generalizability of the findings, Human Renal Proximal Tubule Epithelial (HK-2) cells were used. HK-2 is an immortalized cell line with minimal variation between passages and batches; they are currently widely used in the establishment of oxidative stress models (17). HK-2 cells were cultured in F12 medium containing 10% FBS under standard conditions of 5% CO_2 and 37˚C. After the cells adhered, the medium was replaced with medium containing 0.8 mM H_2O_2 to treat the cells for 24 h, followed by a 48-h recovery period in medium containing Crocin I or no drug.

CCK-8 cell viability assay. Cell viability was detected using the CCK-8 kit as follows: WI-38 cells were seeded at a density of $1x10^4$ cells/well in a 96-well culture plate. After 24 h of culture, different concentrations of Crocin I (1, 2, 5, 10, 20, 40 μM) were added to each well, with 6 parallel wells set for each concentration. After 3 days of culture with Crocin I treatment, 10 μl of CCK-8 solution was added to each well, and the cells were cultured at 37˚C with 5% CO_2 for 1-2 h. The absorbance value was measured using an enzyme reader at 450 nm, and the relative cell viability was calculated, with the viability of the blank group without drugs set as 100%.

SA-β-Gal staining. SA-β-Gal staining was detected by SA-β-Gal staining kit. Cells were treated according to the indicated experiments and the supernatant was removed. Then, the fixation solution from the kit was added and incubated at room temperature for 15 min. After washing with PBS, the staining solution was added and the cells were incubated with the staining solution at 37˚C for 3-16 h. The positive cells appeared blue-green after staining. After staining, the cells were counted and observed under a microscope.

Western blotting. The cells were lysed with RIPA lysis buffer (cat no. P0013B; Beyotime Biotechnology) to extract total protein. The protein concentration was determined by a BCA

assay, and the loading buffer was prepared. A total of 20 μg of protein were added to each well for SDS-PAGE using 10% gels. The separated proteins were transferred onto a PVDF membrane, and the membrane was blocked with 5% skimmed milk in TBST (Tris-Borate-Sodium Tween-20) for 1 h at 4˚C. Then, the PVDF membrane was incubated with the primary antibodies (dilution, 1:1,000) overnight at 4˚C. The next day, the PVDF membrane was incubated with the secondary antibodies (HRP-conjugated Goat anti-Rabbit IgG, cat no. AS014, Abclonal Biotech Co., Ltd.; and HRP-conjugated Goat anti-Mouse IgG, cat no. AS003, Abclonal Biotech Co., Ltd.; both at 1:1,000 dilution) at room temperature for 1 h. Finally, chemiluminescence enhancement technique (Super ECL Detection Reagent; Shanghai Yeasen Biotechnology Co., Ltd.) was used for color development.

Quantitative PCR. Total RNA was extracted using the QIAamp DNA Mini Kit (cat no. 51304; Qiagen GmbH). The reverse transcription experiment was performed using the SuperScript™ IV First-Strand Synthesis System Kit (cat no. 18091050; Invitrogen; Thermo Fisher Scientific, Inc.). The primer sequences were synthesized by Beijing Qingke Biotechnology Co., Ltd., and are shown in Table I. For reverse transcription, the mixed sample was preheated at 37˚C for 15 min, then heated to 85˚C for 5 sec, and finally cooled to 4˚C and held at that temperature. The samples were mixed with SYBR Green I (cat no. S7563; Thermo Fisher Scientific, Inc.), and the expression of the PKM gene was quantified using the real-time PCR system LightCycler 480 [Roche Diagnostics (Shanghai) Co., Ltd.]. qPCR was performed under the following thermal cycling conditions: Initial hold at 95˚C for 5 min, followed by 40 cycles of denaturation at 95˚C for 10 sec and annealing at 60˚C for 30 sec. Gene expression levels were defined by threshold cycles, and data analysis was performed using the $2^{-\Delta\Delta Cq}$ method (18). The primers required for the present study are shown in Table I.

ROS analysis. Cells to be tested were washed with PBS, then incubated with DMEM containing 10 μM reactive oxygen free radical fluorescent probe (DCFH-DA; Beyotime Biotechnology) for 20 min in a 37˚C incubator. Cells washed with DMEM, digested with trypsin, centrifuged to collect cells and resuspend in PBS. The intracellular ROS content was detected using a BD FACSCanto Flow Cytometer (Waters Biosciences).

RNA sequencing (RNA-seq) analysis. Total RNA was extracted from WI-38 cells utilizing TRIzol™ reagent (cat no. 15596026; Thermo Fisher Scientific, Inc.) according to the manufacturer's procedure. RNA sequencing, data processing and analysis were outsourced to LC-Bio Technologies Co., Ltd. (project no. LC-P20260525063), following these steps: The total RNA quantity and purity were analyzed by Thermo Fisher Qubit3.0 (Q33216; Thermo Fisher Scientific, Inc.) and Agilent 5300 Fragment Analyzer (M5311AA; Agilent Technologies, Inc.). High-quality RNA samples with RNA integrity number >7.0 were used to construct the sequencing library, followed by quantification on a NanoDrop ND-1000 (concentration >50 ng/μl, total amount >1 μg). Library construction involved two rounds of polyadenylated [poly(A)] mRNA enrichment using oligo(dT) magnetic beads (Thermo Fisher Scientific, Inc.). mRNA was fragmented at 94˚C for 6 min (NEBNext Magnesium RNA Fragmentation Module; E6150; New England BioLabs, Inc.), then reverse-transcribed to cDNA using SuperScript II Reverse Transcriptase. During second-strand synthesis, double-stranded cDNA was constructed by incorporating dUTP (Thermo Fisher Scientific, Inc.) with *E. coli* DNA Polymerase I and RNase H (both New England BioLabs, Inc.). After end repair and adapter ligation, strand-specific libraries were prepared via UDG enzyme (New England BioLabs, Inc.) digestion. Final libraries (300±50 bp) were amplified through 8 PCR cycles (98˚C/15, 60˚C/15 and 72˚C/30 sec). Sequencing was performed on the Illumina Novaseq™ X Plus (Novaseq X Plus; Illumina, Inc.) in 150-bp paired-end mode. Raw data were processed by fastp to remove adapter sequences and low-quality bases, followed by alignment to the human reference genome GRCh38 using HISAT2. Transcript assembly and FPKM quantification were conducted with StringTie. Differentially expressed genes (DEGs) were identified by DESeq2 analysis (|log₂ fold change| >1, adjusted P<0.05).

Table I. Quantitative PCR primers.

Primer name	Primer sequence (5'-3')
PKM-F	ATTATTTGAGGAACTCCGCCGCCT
PKM-R	ATTCCGGGTCACAGCAATGATGG
GAPDH-F	CTGTTGCTGTAGCCAAATTCGT
GAPDH-R	ACCCACTCCTCCACCTTTGAC

F, forward; R, reverse.

Molecular docking. The Crocin I compound was docked with the potential target to analyze their binding affinities. The crystal structure of the PKM2 protein (PDB ID: 9HIC) was downloaded from the RCSB Protein Data Bank (http://www.pdb.org/), and then the Crocin I MOL.2 format was downloaded from the TCMSP database (https://www.tcmsp-e.com/molecule.php?qn=1405). Both the protein and Crocin I structures were modified using the Autodock tools 1.5.6 software (https://autodock.scripps.edu/), including water removal, hydrogen and Kollman charges addition. Both the modified files were saved in pdbqt format. And then, Autodock Vina was used for docking. The final docking result was visualized by using PyMOL 3.1 software (https://www.pymol.org/).

PK activity analysis. The PK activity assay kit was used to measure PKM2 enzyme activity. After removing the culture medium from the cells to be tested, the cells were washed once with PBS, then extraction buffer (1 ml of extraction buffer per $5x10^6$ cells) was added. The cells were scraped off and collected into a centrifuge tube. The solution containing the cells was then sonicated on an ice bath with the following setting: Power 200 W, sonicate for 3 sec, pause for 10 sec and repeat 30 times. This was then centrifuged at 8,000 x g and 4˚C for 10 min, and once this was complete the supernatant was collected and placed on ice until ready for analysis. The microplate reader

was preheated to 37˚C for 30 min. Then 10 μl of sample, 10 μl of Reagent 3 and 180 μl of buffer, were mixed well, and the absorbance (A1) was quickly measured at 37˚C and 340 nm. The absorbance (A2) was then measured again after 2 min. ΔA=A1-A2 was calculated based off of these readings.

PK activity was calculated using the following formula: PK activity ($U/10^4$ cell)=[ΔAxV1/(εxd)/10^9]÷(NxV2/V3)/T. Definition of the units: One enzyme activity unit is defined as the consumption of 1 nmol of NADH per minute per $1x10^4$ cells in the reaction system; V1, total volume of the reaction system, $2x10^{-4}$ L; ε, molar extinction coefficient of NADH, $6.22x10^3$ l/mol/cm; d, path length of the 24-well plate, 1.5 cm; V2, volume of sample added (0.01 ml); V3, volume of extraction solution added, (1 ml); T, reaction time (2 min); N, total number of cells (10^4).

L-lactate production rate analysis. The test was conducted using the L-LA content detection kit. The procedure was performed according to the manufacture's instructions. The cells were collected and suspended in 1 ml of extraction solution 1 at a concentration of $5x10^6$ cells/ml. After ultrasonic disruption, the mixture was centrifuged at 12,000 x g for 10 min at room temperature. A total of 0.8 ml was pipetted from the supernatant and 0.15 ml of extraction solution 2 was added. Then, the mixture was centrifuged at 12,000 x g for 10 min at room temperature. The supernatant was pipetted for testing. The working solutions 2, 4 and 5 were added to the sample and were mixed thoroughly. Then, use the absorbance value was recorded at 570 nm.

The L-LA content was calculated using the following formula: LA content (μmol/ml)=C1xΔ1/Δ2x(V1+V2)/[V4xV1/(V3+V4)] xF. The definitions are as follows: C1, standard concentration (2 μmol/ml); Δ1=test group-blank group; Δ2=standard group-blank group; V1, volume of supernatant (0.8 ml); V2, volume of extract 2 (0.15 ml); V3, volume of extract 1 (1 ml); V4, volume of liquid sample (0.1 ml); F, dilution factor.

Statistical analysis. All experimental results were independently repeated three times. Data are presented as the mean ± standard deviation. All data were analyzed and plotted using Graph Pad 8.4.3 (Dotmatics). One-way analysis of variance (ANOVA) was used for comparisons among multiple groups supplemented with a Dunnett's post hoc test (suitable for comparing multiple experimental groups to a single control group) and Tukey's post hoc test (suitable for pairwise comparisons among all groups). $P<0.05$ was considered to indicate a statistically significant difference.

Results

Effect of Crocin I on replicative senescence of WI-38 cells. As shown in Fig. 1B, 30PD WI-38 cells treated with Crocin I for 3 days showed an increased cell viability in the dose of 5, 10, 20, 40 μM, with 10 μM showing an optimal efficacy. This concentration was then selected for further long-term culture of WI-38 cells. Starting from 30PD, a solvent control group (0.1% DMSO) and a dosing group (10 μM Crocin I) were established to culture WI-38 cells. The cells were then cultured by the conventional method until 55PD. Compared with the young cells at 30PD, the SA-β-Gal staining positive rate in the solvent control group at 55PD was ~90%, while it was significantly lower in 10 μM Crocin I treated group than that of the solvent control group at 55PD (Fig. 1C and D). Meanwhile, compared with 55PD control group, the intracellular ROS levels were significantly decreased in the Crocin I treatment group (Fig. 1E and F); a decrease in intracellular ROS levels indicates reduced oxidative stress (19). Furthermore, western blotting analysis revealed that the expression of the aging-related proteins p53 and p21 was significantly lower in the Crocin I group than that of the solvent control group, low expression levels similar to those in young cells, shown as in Fig. 1G, H and I. The above results indicate that Crocin I reduces intracellular ROS levels and oxidative stress, and induces a decrease in p53/p21 expression, resulting in delayed cellular senescence.

To determine whether Crocin I has similar effects in other cell lines, HK-2 cells were selected for further experiments. HK-2 is an immortalized cell line that can be induced to undergo premature senescence by 0.8 mM H_2O_2 (20). As shown in Fig. S1A, Crocin I exhibited no cytotoxicity toward HK-2 cells; therefore, the same concentration (10 μM) was used, as in the previous experiments. After treating HK-2 cells with 0.8 mM H_2O_2 for 24 h, the medium was replaced with fresh medium containing 10 μM Crocin I, and the cells were allowed to recover for 24 h. As shown in Fig. S1B, the SA-β-Gal staining positivity rate was significantly increased in H_2O_2-treated HK-2 cells, while Crocin I effectively reduced this positivity rate. Furthermore, Crocin I inhibited the H_2O_2-induced increase in p53 and p21 protein expression levels (Fig. S1C-E).

Effect of Crocin I on premature senescence induced by AAPH. In order to explore the effect of Crocin I on cells senescence a premature senescent cell model in WI-38 cells induced by AAPH, a reagent widely used for the induction of premature senescence, was used (21). The present results showed that AAPH ranged 3-5 mM induced a robust decline of cell viability ≤50% (Fig. 2A). Moreover, there was no significant difference in the rate of positive of SA-β-Gal staining induced by AAPH among 4 and 5 mM (Fig. 2B, C, D and G). Therefore, AAPH at 4 mM was then chosen to construct the premature cellular senescence model for the subsequent experiments. After AAPH treatment of 30PD WI-38 cells for 24 h, the medium was replaced with fresh medium containing each concentration of Crocin I (5, 10, 20 μM) for 3 days of recovery. N-acetylcysteine reduces intracellular ROS levels and serves as a positive control at a concentration of 2 mM (22). As shown in Fig. 2E and F, the results of SA-β-Gal staining showed that the intervention of Crocin I (5, 10, 20 μM) effectively reduced the positive rate of staining. In addition, Crocin I dose-dependently suppressed the elevation of p53 and p21 protein expressions induced by AAPH (Fig. 2H and I).

Effect of Crocin I on SIRT1/PKM2 expression and lactate production in late PD WI-38 cells. For further discovery of potential target molecules for Crocin I intervention in cellular senescence, RNA-seq analysis was performed. As shown in the Fig. 3A, Crocin I intervention induced genes alteration in genes such as pyruvate kinase (pyruvate kinase M1/2 type, PKM) as well as other genes. As shown in Fig. 3B and C, gene ontology

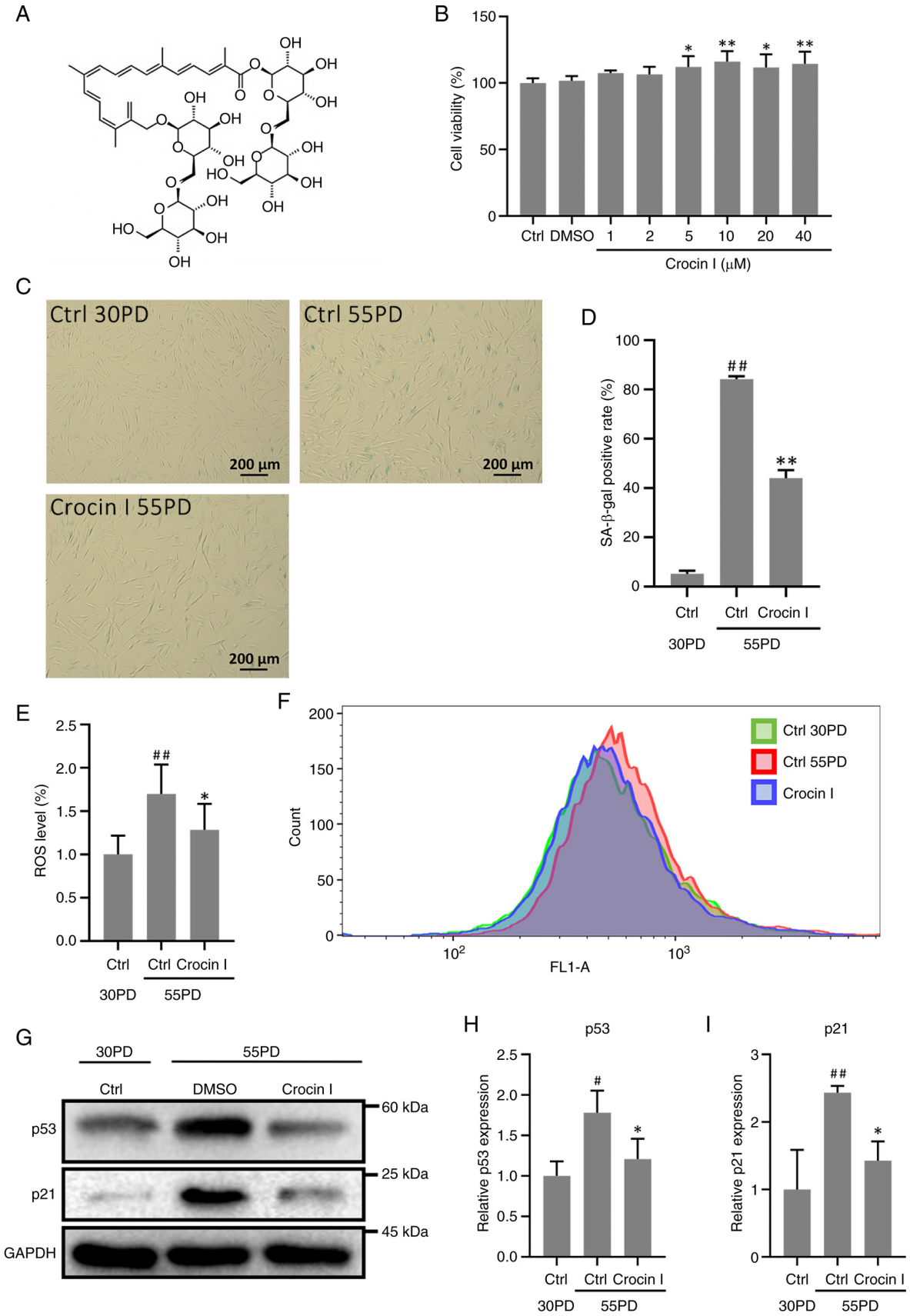

Figure 1. Effect of Crocin I on replicative senescence of WI-38 cells. (A) The chemical structure formula of Crocin I. (B) The effect of Crocin I on the viability of WI-38 cells detected by the cell counting kit-8 assay. (C and D) The effect of Crocin I (10 μM) on the positive rate of SA-β-Gal staining in WI-38 cells after long-term dosing culture. All cells were observed under a 10x objective lens. (E and F) The change in ROS levels in WI-38 cells after long-term dosing culture with Crocin I. Count: quantity of cell; FL1-A: Fluorescence Channel 1 Area. (G, H, I) The change in senescence-related proteins in WI-38 cells after long-term dosing culture with Crocin I. Ctrl 30PD: Young control group, 30PD cells; Ctrl 55PD: Solvent control group, 30PD cells cultured with 0.1% DMSO until 55PD; Crocin I: Dosing group, 30PD cells cultured with 10 μM Crocin I until 55PD. $^{\#\#}$P<0.01 vs. Ctrl 30PD; $^{\#}$P<0.05 vs. Ctrl 30PD; **P<0.01 vs. Ctrl 55PD; *P<0.05 vs. Ctrl 55PD. ROS, reactive oxygen species; SA-β-Gal, senescence-associated β-galactosidase.

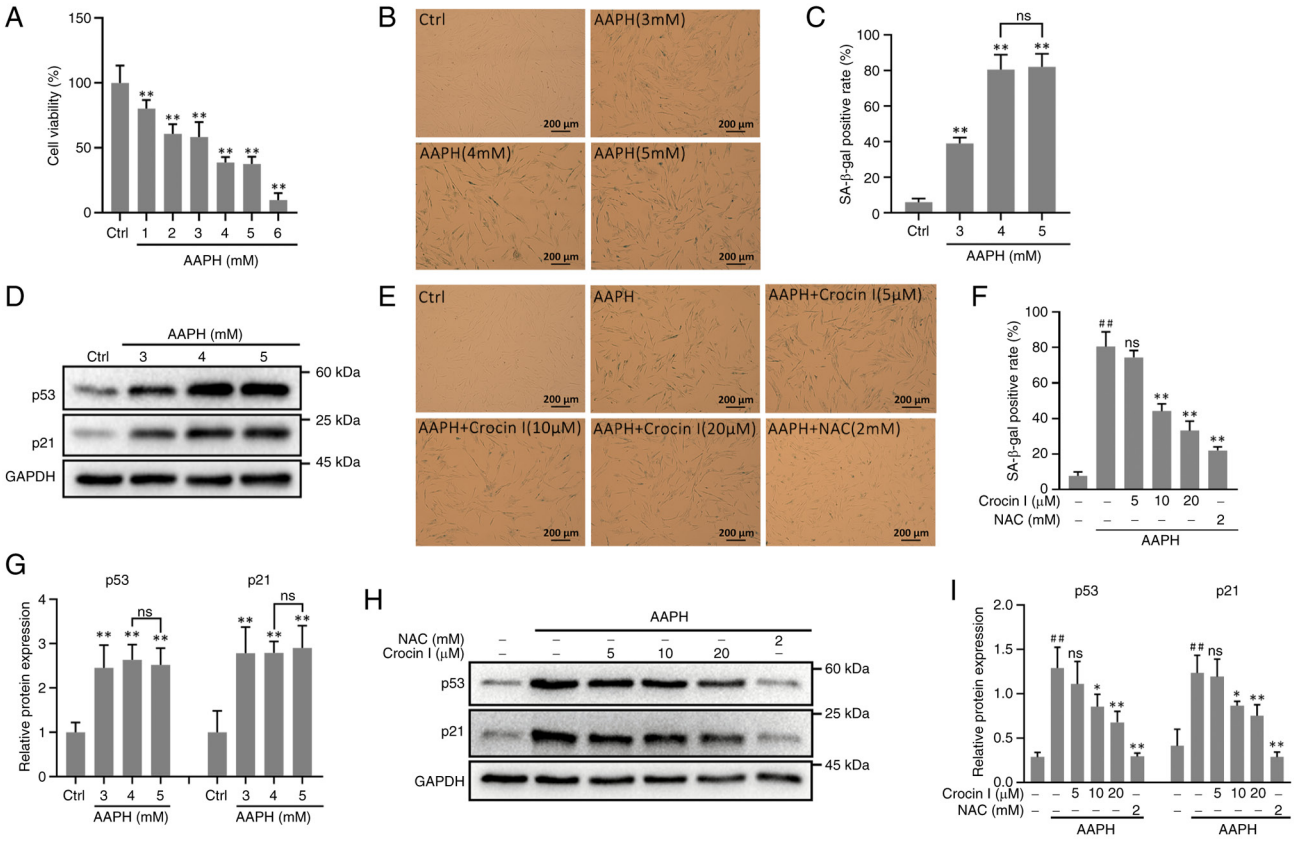

Figure 2. Effect of Crocin I on premature senescence induced by AAPH. (A) The effect of AAPH on the viability of WI-38 cells was detected by the cell counting kit-8 assay. The cell viability decreased within the range of 3-5 mM and showed more significant inhibitory effect at 4-5 mM. (B and C) 30PD WI-38 cells were treated with AAPH (3-5 mM) and recovered for 3 days and detected by SA-β-Gal staining. All cells were observed under a 10x objective lens. (D and G) 30PD WI-38 cells were treated with AAPH (3-5 mM) and recovered for 3 days to detect senescence-related molecules by western blotting. (E and F) Inhibitory effects of Crocin I on AAPH-induced (4 mM) increment of SA-β-Gal activity. All cells were observed under a 10x objective lens. (H and I) The effect of Crocin I on AAPH-induced (4 mM) increased expression of p53 and p21. 30PD WI-38 cells were treated with the AAPH (4 mM) for 24 h and then cultured for 3 days by replacing the medium containing each concentration of Crocin I or NAC. ($^{\#\#}$P<0.01, vs. Ctrl; **P<0.01, vs. AAPH only; *P<0.05, vs. AAPH only). Ns, not significant; SA-β-Gal, senescence-associated β-galactosidase; AAPH, 2,2'-azobis-2-methy-propanimidamide dihydrochloride.

(GO) analysis indicated that the differentially expressed genes induced by Crocin I at the dose of 10 μM were enriched in GO terms such as 'phosphorylation', 'oxidoreductase activity', 'glucose metabolic process' and 'replicative senescence'. In addition, KEGG analysis revealed that the differentially expressed genes were enriched in 'glycolysis/gluconeogenesis', 'hippo signaling pathway' and 'pyruvate metabolism'. As emphasized by Gorgoulis *et al* (23), cellular senescence not only involves DNA damage responses and protein stress but is also frequently accompanied by metabolic shifts towards glycolysis. While the PKM gene was mainly involved in the process of glycolysis, which could encode two forms of enzymes, M1 and M2 (24). Compared with the solvent control group, PKM gene expression was significantly decreased in the Crocin I group (Fig. 3A and D). Meanwhile, molecular docking between PKM2 and Crocin I was performed, which demonstrated that the binding energy was -8.3 kJ/mol. As shown in Fig. 3E, Crocin I mainly interacts with PKM2 at the residues VAL508, CYS424 and ASP160. To verify whether Crocin I binding affects PKM2 enzyme activity, a PK enzyme activity assay was conducted. A kit for detection of total PK enzymatic activity (PKM1 and PKM2) was used. The experiment was designed using the PKM2 inhibitor shikonin to detect the effect of Crocin I on PKM1 or PKM2 enzymatic activity. Previous studies have shown that 5 μM Shikonin markedly inhibits intracellular PKM2 enzymatic activity (25); therefore, cells were co-treated with Shikonin and Crocin I to determine whether Crocin I inhibits PKM1 enzymatic activity. As shown in Fig. 3F, compared with the with Shikonin alone treatment group, co-treatment with Shikonin and Crocin I did not further reduce the overall enzymatic activity of pyruvate kinase, demonstrating that the inhibitory effect of Crocin I on PKM1 was undetectable in current experiment. While Crocin I alone induced an obvious reduction on PKM2 enzymatic activity. Additionally, Crocin I was found to suppress the expression level of PKM2 by western blotting (Fig. 3G and H). Moreover, significantly lower levels of lactate were observed after Crocin I intervention (Fig. 3K), suggesting a reduced contribution of glycolysis during the cellular senescence. A previous study has confirmed that SIRT1 interacts with and deacetylates PKM2 at K135 and K206, thus leading to reduced PKM2 enzyme activity and lactate production (26). Consistently, the present study also illustrated that Crocin I intervention could enhance the level of SIRT1 expression (Fig. 3I and J), revealing that Crocin I intervention may improve cellular senescence through SIRT1/PKM2 mediated glycolysis pathway. Moreover, the inhibition of Crocin I on the PKM2 protein expression was partly reversed by sirtinol (Fig. 3L, M and N), an inhibitor

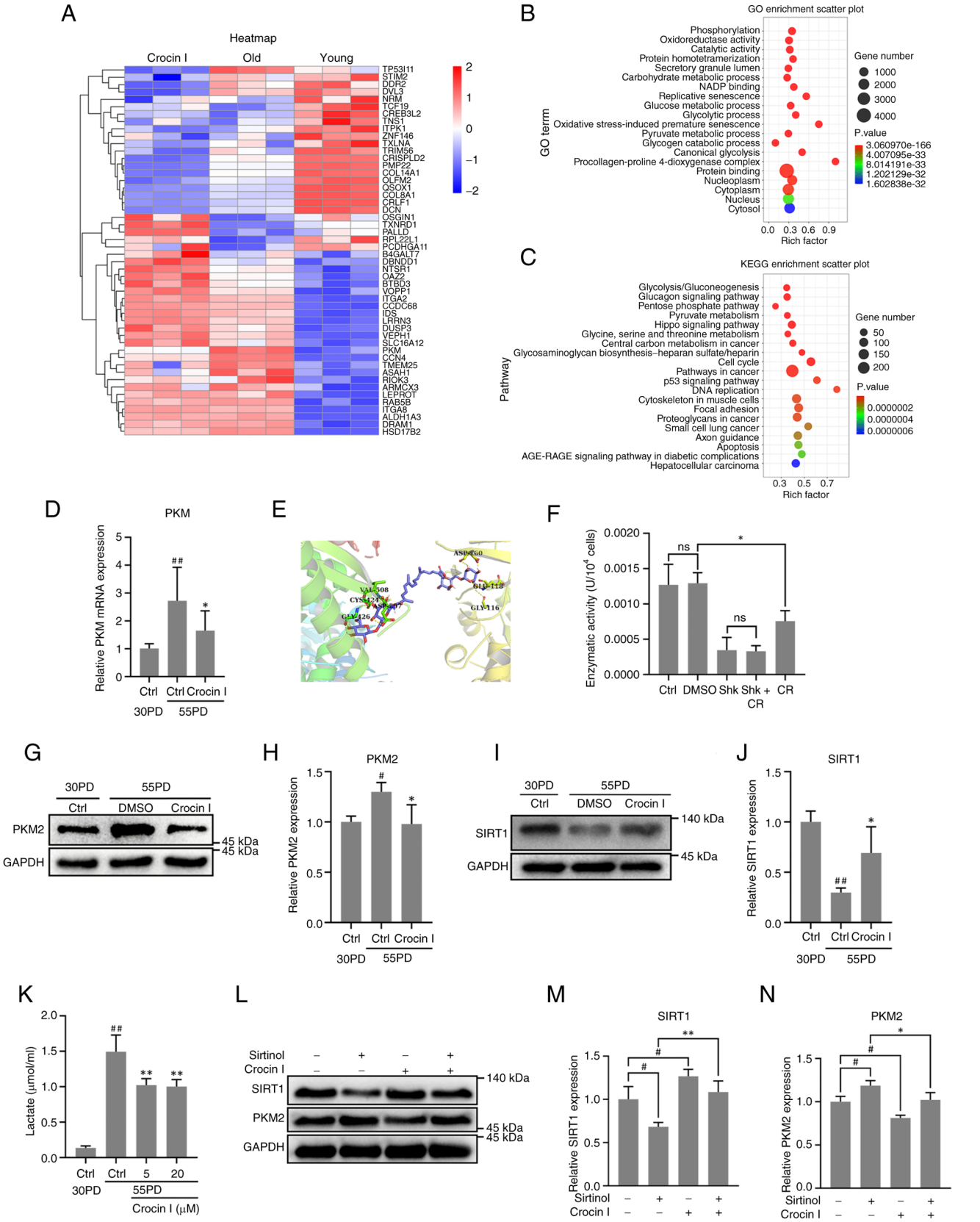

Figure 3. Effect of Crocin I on SIRT1/PKM2 expression and lactate production in late PD WI-38 cells. (A) Heatmap of the gene expression changes in WI-38 cells. Young: 30PD cells; Old: 55PD cells; Crocin I: 55PD cells treated with 10 μM Crocin I for 48 h. (B) GO and (C) KEGG enrichment analysis of alteration genes. (D) Effect of Crocin I on expression level of PKM gene in 55PD WI-38 cells. (E) Molecular docking of PKM2 protein and Crocin I predicted by Autodock tools. (F) Effect of Crocin I on PK enzyme activity. PK enzyme activity was measured after 30PD WI-38 cells were treated with the respective drugs (Shk 5 μM; CR 10 μM) for 24 h. (G and H) Effect of Crocin I on PKM2 protein expression in 55PD WI-38 cells. (I and J) Effect of Crocin I on SIRT1 protein expression in 55PD WI-38 cells. (K) Effect of Crocin I on lactate content in senescent WI-38 cells. (L-N) The effect of Crocin I on SIRT1 and PKM2 protein expression in WI-38 cells after Sirtinol treatment (Sirtinol 10 μM; Crocin I 10 μM). WI-38 cells were pretreated with Sirtinol for 4 h, followed by treatment with Crocin I for 24 h. ($^{\#\#}$P<0.01, vs. Ctrl 30PD; $^{\#}$P<0.05, vs. Ctrl 30PD; **P<0.01, vs. Ctrl 55PD; *P<0.05, vs. Ctrl 55PD). Shk, Shikonin; CR, Crocin I; GO, gene ontology; KEGG, Kyoto encyclopedia of genes and genomes; PK, pyruvate kinase.

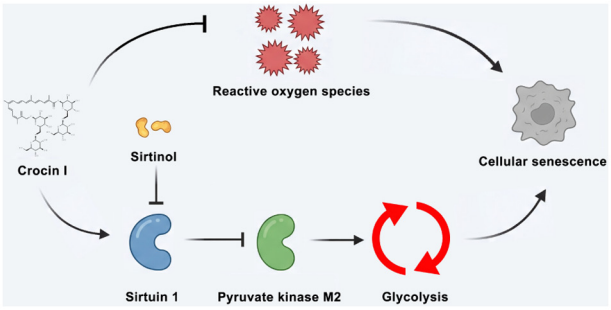

Figure 4. Schematic diagram of the mechanism by which Crocin I delays senescence. Treatment with Crocin I reduced intracellular reactive oxygen species levels, alleviated oxidative stress, and delayed cellular senescence; at the same time, Crocin I treatment increased sirtuin 1 levels, which in turn reduced pyruvate kinase M2 activity, thereby decreasing glycolytic activity and delaying cellular senescence.

of SIRT1 (27), which indicated that Crocin I could directly regulate PKM2 expression via SIRT1, at least in part. A schematic diagram of the delays senescence mechanism of Crocin I is shown in Figure 4.

Discussion

Saffron (*Crocus sativus L.*) has a wide range of biological properties with multiple applications in different industrial sectors as pharmaceuticals and nutrients (28,29). Currently, the commercial production of Crocin is based on purification from saffron stigmas and gardenia fruits (30). Moreover, saffron is not only used as a classical TCM but also universally recognized as a safe and valuable spice (31). For instance, it is used as dietary supplement in the culinary traditions in European, Middle Eastern and Asian countries (32). Ouahhoud *et al* (33) had revealed that saffron stigmas exhibited vigorous biological activity, with an IC50 value of 1,554.37 μg/ml. In addition, administration of a high dose of Crocin (150 mg/kg) to tumor-bearing mice showed no reported adverse toxic effects. Thus, it is a safe drug at an average dose, but an overdose of Crocin exhibited adverse effect including nausea, vomiting, stomach upset, dizziness, constipation, restlessness, headaches, collapse, liver and kidney impairments (34). Cytotoxic effect analysis showed an IC50 of 20 μM in HeLa cells (34). In the present study, the effect of Crocin I against cellular senescence both in replicative senescence model and AAPH-induced premature cellular senescence model was preliminarily explored. It was found that Crocin I could significantly reduce the protein levels of the aging-related molecular p53 and p21 in the WI-38 cells; meanwhile, Crocin I suppressed the production of intracellular ROS. PKM was further identified as the potential target molecule of Crocin I intervention during cellular senescence, following with enhancing of the level of SIRT1 expression. Furthermore, Crocin I significantly reduced the level of cellular lactate in late PD fibroblasts, indicating that Crocin I may regulate the level of glycolysis to alleviate cellular senescence.

Cellular senescence is a dynamic biological process illustrated by a gradual decline in multiple cellular activities, resulting to the whole-body aging as well as age-related diseases (35). Notably, the dysfunction in glucose metabolism, such as enhanced glycolysis and alteration in glucose transporter activity, are frequently observed in senescent cells (36). For instance, vascular endothelial cells (ECs) undergo changing metabolic reprogramming, including glycolysis, redox homeostasis alteration, mitochondrial dysfunction following with body aging (37). On the other hand, healthy ECs commonly maintain metabolic homeostasis primarily relying on the energy provided by glycolysis pathway (37). Glycolysis process could enhance the production of lactic acid by producing pyruvate relying on the high level of lactate dehydrogenase (LDH), PKM and hexokinase (38). While PKM is responsible for the last conversion step of glycolysis to produce pyruvate (39). Meanwhile, the enhanced of LDH resulted by PKM produced a higher level of lactate in senescent cells than young cells (40), leading to multiple senescence-associated events, such as cancers and evasion of immune responses (41,42). In addition, the PKM gene encodes two forms of proteins, PKM1 and PKM2 (43), and PKM2 also exists two forms, dimer and tetramer, each with distinct biological functions (44). The dimer form can enter the cell nucleus to participate in regulation and serves as a switch for energy metabolism and substance synthesis; the tetramer form mainly functions as an enzyme to regulate glycolysis (45). Consistent with previous studies, it was observed in the present study that elevating the level of PKM2 enhanced glucose metabolism through increasing production of lactate in those senescent cells, while Crocin I treatment partly decreased the levels of PKM2 and lactate which may result in delaying senescence.

Beside to the regulation on glycolysis of Crocin I, the RNA seq data indicated several other pathways including Hippo signaling and pyruvate metabolism. The Hippo pathway is an evolutionarily conserved signaling cascade pathway to regulate tissue growth and cell fate (46-48), including cell differentiation, proliferation as well as cell senescence. For example, YAP and its paralog, TAZ are well-known transcriptional coactivators that activate transcription in Hippo pathway. YAP can transcriptionally regulate cyclin D-dependent kinase 6 gene expression to maintain normal cell growth and suppress cellular senescence (49). These results suggest that Crocin I delays cellular senescence, possibly via multiple pathways rather than glycolysis pathway specially.

Previous study had indicated that PKM2 had been identified as a downstream target of SIRT1 (26), which is a member of the sirtuin family. SIRT1 is an NAD^+-dependent protein deacetylase (50) to illustrate essential roles in a series of cellular biological processes, including DNA repair, apoptosis, senescence and autophagy (51). Furthermore, SIRT1 has also showed notable function in energy balance through affecting mitochondrial biogenesis, calcium homeostasis and oxidative phosphorylation (52,53). In line with this respect, the present study found that SIRT1 was decreased in senescent WI-38 cells, with a high level of cellular ROS, while Crocin I decreased the level of ROS and enhanced the expression of SIRT1. Moreover, it was observed that PKM2 was decreased in the presence of high expressing of SIRT1. A previous study had indicated that SIRT1 inhibited lactate accumulation through the deacetylation-induced PKM2 inhibition to alleviate neuroinflammation (26). Specifically, SIRT1 could deacetylate two lysine residues of PKM2, K135 and K206, which markedly blocked PKM2 enzyme activity (26). PKM2 is responsible for the first step in manipulating lactate

production, which was consistent with the present finding. However, there is a need to further explore the detailed molecular mechanisms for the interaction between SIRT1 and PKM2 during Crocin I delaying cellular senescence.

Consist with the present study, Crocin also could effectively inhibit the generation of ROS in mouse retinal photoreceptor (661W) cells. In addition, treatment with 200 μM of Crocin could alleviate mitochondrial aggregation and notably prevented an all-trans-retinal (atRAL)-induced decrease in mitochondrial membrane potential levels (54). In addition, Crocin remarkably attenuated an increase in mitochondrial superoxide levels in atRAL-treated 661W cells. Meanwhile, Crocin notably inhibits atRAL-induced apoptosis in photoreceptor cells by reducing damage and oxidative stress (54). A clinical trial showed that 8 weeks of treatment of Crocin capsule is effective in reducing oxidative stress in serum samples and decreasing DNA damage (55).

This study preliminarily proved that Crocin I has the functions of regulating the level of glycolysis and delaying cellular senescence. However, there are still some limitations that remain unresolved. First, it is not known whether Crocin I directly regulates the PKM gene, and its upstream or downstream genes still need further exploration. And molecular docking illustrated that Crocin I could bind with PKM2, however functional assays of PKM2 enzymatic activity was not performed. Second, the association between regulating the level of glycolysis and delaying cellular senescence has not been fully verified, and subsequent work should address this issue. Third, the reduction of PKM2 expression levels was observed, however, the oligomeric state, dimer or tetramer, remains unconfirmed. Lastly, the specific acetylation site(s) of PKM2 regulated by SIRT1 have not been fully identified in the present experimental system.

In conclusion, the present results indicate that Crocin I has an anti-senescence effect. Crocin I regulated PKM2 expression by upregulating SIRT1; since PKM2 is a key molecule in the regulation of glycolysis, this may be one of the factors contributing to the anti-senescence effect. A limitation of the present study is that the specific mechanisms by which Crocin I regulates glycolysis in a cellular senescence model have not yet been thoroughly investigated, and therefore further research is needed.

Acknowledgements

Not applicable.

Funding

The present study was supported by the project from the Traditional Chinese Medicine Administration of Zhejiang Province (grant no. 2025ZL161) and Joint TCM Science & Technology Project of National Demonstration Zones for Comprehensive TCM Reform (grant no. GZY-ZJ-KJ-24055).

Availability of data and materials

The RNA-seq data generated in the present study may be found in the Gene Expression Omnibus database under accession number GSE335498 or at the following URL: https://www.ncbi.nlm.nih.gov/geo/query/acc.cgi?acc=GSE335498. The other data generated in the present study may be requested from the corresponding author.

Authors' contributions

YF designed the present research and wrote the original manuscript draft. ZD and CW analyzed the experimental data. YC developed the methodology. SW participated in the conception and design of the study and provided guidance. GM reviewed and edited the manuscript, supervised the project, acquired funding and contributed to the conceptualization of the study. HS acquired funding and contributed to the conceptualization of the study. YF, ZD, CW, YC, SW and GM confirm the authenticity of all the raw data. All authors have read and approved the manuscript.

Ethics approval and consent to participate

Not applicable.

Patient consent for publication

Not applicable.

Competing interests

The authors declare that they have no competing interests.

References

1. Birch J and Gil J: Senescence and the SASP: Many therapeutic avenues. Genes Dev 34: 1565-1576, 2020.
2. Kroemer G, Maier AB, Cuervo AM, Gladyshev VN, Ferrucci L, Gorbunova V, Kennedy BK, Rando TA, Seluanov A, Sierra F, *et al*: From geroscience to precision geromedicine: Understanding and managing aging. Cell 188: 2043-2062, 2025.
3. Zhu Y, Liu X, Ding X, Wang F and Geng X: Telomere and its role in the aging pathways: Telomere shortening, cell senescence and mitochondria dysfunction. Biogerontology 20: 1-16, 2019.
4. Mas-Bargues C: Mitochondria pleiotropism in stem cell senescence: Mechanisms and therapeutic approaches. Free Radic Biol Med 208: 657-671, 2023.
5. Gao Y, Shen S, Wang Y and Tian M: Organ crosstalk: The role of spleen. Phenomics 5: 192-207, 2024.
6. Yang YN, Zhan JG, Cao Y and Wu CM: From ancient wisdom to modern science: Gut microbiota sheds light on property theory of traditional Chinese medicine. J Integr Med 22: 413-444, 2024.
7. Cai M, Guo Q, Li J, Dai X, Su H, Zhang W, Qiang N, Li G, Jin Z and Zhu H: Resveratrol attenuates H_2O_2-induced aging and apoptosis in mouse hippocampal neuron HT22 cells by activating autophagy via the SIRT1/FoxO1 signaling pathway. Mol Neurobiol 63: 12, 2025.
8. Javadi B, Sahebkar A and Emami SA: A survey on saffron in major islamic traditional medicine books. Iran J Basic Med Sci 16: 1-11, 2013.
9. Geng Lei WG, Liu Shaoqing: Optimization on formula parameters of *Crocus sativus* oral liquid by response surface methodology and its anti-fatigue function. Food Sci Technol 43: 156-160, 2018.
10. Karkoula E, Dagla IV, Baira E, Kokras N, Dalla C, Skaltsounis AL, Gikas E and Tsarbopoulos A: A novel UHPLC-HRMS-based metabolomics strategy enables the discovery of potential neuroactive metabolites in mice plasma, following i.p. administration of the main *Crocus sativus L.* bioactive component. J Pharm Biomed Anal 177: 112878, 2020.
11. Pourmousavi L, Asadi RH, Zehsaz F and Jadidi RP: Potential therapeutic effects of crocin. Naunyn Schmiedebergs Arch Pharmacol 397: 7395-7420, 2024.

12. García-Ricote I, Jiménez AJL, Megías D, Gavira-O Neill CE, Gómez-Gómez L, Ahrazem O and Casas-Tintó S: Protective effects of crocin-enriched tomato in ageing and brain mitochondrial function using *Drosophila melanogaster*. Biomed Pharmacother 196: 119119, 2026.
13. Heidari S, Mehri S, Shariaty V and Hosseinzadeh H: Preventive effects of crocin on neuronal damages induced by D-galactose through AGEs and oxidative stress in human neuroblastoma cells (SH-SY5Y). J Pharmacopuncture 21: 18-25, 2018.
14. Wang Q, Zhang L, Su H and Wan X: Effect of saffron on antioxidant capacity of D-galactose-induced aging rat model. Chin Arch Tradit Chin Med 38: 18-21, 2020.
15. Legrain Y, Touat-Hamici Z and Chavatte L: Interplay between selenium levels, selenoprotein expression, and replicative senescence in WI-38 human fibroblasts. J Biol Chem 289: 6299-6310, 2014.
16. Mao G, Li H, Ding X, Meng X, Wang G and Leng SX: Suppressive effects of sirtinol on human cytomegalovirus (hCMV) infection and hCMV-induced activation of molecular mechanisms of senescence and production of reactive oxygen species. Mech Ageing Dev 158: 62-69, 2016.
17. Kim HY, Park JS, Jeon BH, Choi HS, Kim CS, Ma SK, Kim SW and Bae EH: Role of APE1/Ref-1 in hydrogen peroxide-induced apoptosis in human renal HK-2 cells. Kidney Res Clin Pract 43: 186-201, 2024.
18. Livak KJ and Schmittgen TD: Analysis of relative gene expression data using real-time quantitative PCR and the 2(-Delta Delta C(T)) method. Methods 25: 402-408, 2001.
19. Schieber M and Chandel NS: ROS function in redox signaling and oxidative stress. Curr Biol 24: R453-R462, 2014.
20. Rattananinsruang P, Noonin C, Yoodee S and Thongboonkerd V: Comparative analysis of markers for H_2O_2-induced senescence in renal tubular cells. Environ Toxicol Pharmacol 97: 104039, 2023.
21. Tang D, Yan R, Sun Y, Kai G, Chen K and Li J: Material basis, effect, and mechanism of ethanol extract of Pinellia ternata tubers on oxidative stress-induced cell senescence. Phytomedicine 77: 153275, 2020.
22. Kalyanaraman B: NAC, NAC, Knockin' on Heaven's door: Interpreting the mechanism of action of N-acetylcysteine in tumor and immune cells. Redox Biol 57: 102497, 2022.
23. Gorgoulis VG, Pefani DE, Pateras IS and Trougakos IP: Integrating the DNA damage and protein stress responses during cancer development and treatment. J Pathol 246: 12-40, 2018.
24. Zhang Z, Deng X, Liu Y, Liu Y, Sun L and Chen F: PKM2, function and expression and regulation. Cell Biosci 9: 52, 2019.
25. Chen J, Xie J, Jiang Z, Wang B, Wang Y and Hu X: Shikonin and its analogs inhibit cancer cell glycolysis by targeting tumor pyruvate kinase-M2. Oncogene 30: 4297-4306, 2011.
26. Lian B, Zhang J, Yin X, Wang J, Li L, Ju Q, Wang Y, Jiang Y, Liu X, Chen Y, *et al*: SIRT1 improves lactate homeostasis in the brain to alleviate parkinsonism via deacetylation and inhibition of PKM2. Cell Rep Med 5: 101684, 2024.
27. Wang J, Kim TH, Ahn MY, Lee J, Jung JH, Choi WS, Lee BM, Yoon KS, Yoon S and Kim HS: Sirtinol, a class III HDAC inhibitor, induces apoptotic and autophagic cell death in MCF-7 human breast cancer cells. Int J Oncol 41: 1101-1109, 2012.
28. Ali A, Yu L, Kousar S, Khalid W, Maqbool Z, Aziz A, Arshad MS, Aadil RM, Trif M, Riaz S, *et al*: Crocin: Functional characteristics, extraction, food applications and efficacy against brain related disorders. Front Nutr 9: 1009807, 2022.
29. Guo ZL, Li MX, Li XL, Wang P, Wang WG, Du WZ, Yang ZQ, Chen SF, Wu D and Tian XY: Crocetin: A systematic review. Front Pharmacol 12: 745683, 2022.
30. Morote L, Moreno Giménez E, López Jiménez AJ, Rubio-Moraga Á, Aragonés V, Ahrazem O, Daròs JA and Gómez-Gómez L: Biotechnological production of crocetin and crocins using a carotenoid cleavage dioxygenase (CCD4) from Nyctanthes arbor-tristis. Front Plant Sci 16: 1671592, 2025.
31. Abu-Izneid T, Rauf A, Khalil AA, Olatunde A, Khalid A, Alhumaydhi FA, Aljohani ASM, Sahab Uddin M, Heydari M, Khayrullin M, *et al*: Nutritional and health beneficial properties of saffron (*Crocus sativus L*): A comprehensive review. Crit Rev Food Sci Nutr 62: 2683-2706, 2022.
32. Zou Z, Lei D, Wang X, Yin Y, Li H, Di X and Li X: Crocin ameliorates cognitive impairment and pathological changes in Alzheimer's disease model mice by regulating gut microbiota. Food Sci Nutr 13: e71117, 2025.
33. Ouahhoud S, Khoulati A, Kadda S, Bencheikh N, Mamri S, Ziani A, Baddaoui S, Eddabbeh FE, Lahmass I, Benabbes R, *et al*: Antioxidant activity, metal chelating ability and DNA protective effect of the hydroethanolic extracts of *Crocus sativus* stigmas, tepals and leaves. Antioxidants (Basel) 11: 932, 2022.
34. Jiang Z, Gu M, Liu J, Li H, Peng J and Zhang Y: Anticancer activity of crocin against cervical carcinoma (HeLa cells): Bioassessment and toxicity evaluation of crocin in male albino rats. J Photochem Photobiol B 180: 118-124, 2018.
35. Wechter N, Rossi M, Anerillas C, Tsitsipatis D, Piao Y, Fan J, Martindale JL, De S, Mazan-Mamczarz K and Gorospe M: Single-cell transcriptomic analysis uncovers diverse and dynamic senescent cell populations. Aging (Albany NY) 15: 2824-2851, 2023.
36. Mun H, Shin CH, Kim M, Chang JH and Yoon JH: RNA-binding protein AUF1 suppresses cellular senescence and glycolysis by targeting PDP2 and PGAM1 mRNAs. Aging (Albany NY) 17: 1746-1761, 2025.
37. Wang WL, Shih YT, Wei SY and Chiu JJ: Impacts of aging and fluid shear stress on vascular endothelial metabolism and atherosclerosis development. J Biomed Sci 32: 83, 2025.
38. Lund J, Aas V, Tingstad RH, Van Hees A and Nikolić N: Utilization of lactic acid in human myotubes and interplay with glucose and fatty acid metabolism. Sci Rep 8: 9814, 2018.
39. Pan Y, Zheng Q, Ni W, Wei Z, Yu S, Jia Q, Wang M, Wang A, Chen W and Lu Y: Breaking glucose transporter 1/pyruvate kinase M2 glycolytic loop is required for cantharidin inhibition of metastasis in highly metastatic breast cancer. Front Pharmacol 10: 590, 2019.
40. Bhargava P and Schnellmann RG: Mitochondrial energetics in the kidney. Nat Rev Nephrol 13: 629-646, 2017.
41. Lu X, Wu J, Agborbesong E and Li X: P16-positive senescent cells promote DKD by the dysregulation of glycolysis and mitochondrial metabolism. Cell Death Discov 11: 355, 2025.
42. Nacarelli T and Sell C: Targeting metabolism in cellular senescence, a role for intervention. Mol Cell Endocrinol 455: 83-92, 2017.
43. Gupta V and Bamezai RN: Human pyruvate kinase M2: A multifunctional protein. Protein Sci 19: 2031-2044, 2010.
44. Israelsen WJ, Dayton TL, Davidson SM, Fiske BP, Hosios AM, Bellinger G, Li J, Yu Y, Sasaki M, Horner JW, *et al*: PKM2 isoform-specific deletion reveals a differential requirement for pyruvate kinase in tumor cells. Cell 155: 397-409, 2013.
45. Muñoz-Colmenero A, Fernández-Suárez A, Fatela-Cantillo D, Ocaña-Pérez E, Domínguez-Jiménez JL and Díaz-Iglesias JM: Plasma tumor M2-pyruvate kinase levels in different cancer types. Anticancer Res 35: 4271-4276, 2015.
46. Dupont S, Morsut L, Aragona M, Enzo E, Giulitti S, Cordenonsi M, Zanconato F, Le Digabel J, Forcato M, Bicciato S, *et al*: Role of YAP/TAZ in mechanotransduction. Nature 474: 179-183, 2011.
47. Park J and Hansen CG: Cellular feedback dynamics and multilevel regulation driven by the hippo pathway. Biochem Soc Trans 49: 1515-1527, 2021.
48. Harvey KF, Zhang X and Thomas DM: The Hippo pathway and human cancer. Nat Rev Cancer 13: 246-257, 2013.
49. Miyajima C, Nagasaka M, Aoki H, Toriuchi K, Yamanaka S, Hashiguchi S, Morishita D, Aoyama M, Hayashi H and Inoue Y: The Hippo signaling pathway manipulates cellular senescence. Cells 14: 13, 2024.
50. Sauve AA, Wolberger C, Schramm VL and Boeke JD: The biochemistry of sirtuins. Annu Rev Biochem 75: 435-465, 2006.
51. Nakagawa T and Guarente L: SnapShot: Sirtuins, NAD, and aging. Cell Metab 20: 192-192.e1, 2014.
52. Cantó C, Gerhart-Hines Z, Feige JN, Lagouge M, Noriega L, Milne JC, Elliott PJ, Puigserver P and Auwerx J: AMPK regulates energy expenditure by modulating NAD+ metabolism and SIRT1 activity. Nature 458: 1056-1060, 2009.
53. Iwabu M, Yamauchi T, Okada-Iwabu M, Sato K, Nakagawa T, Funata M, Yamaguchi M, Namiki S, Nakayama R, Tabata M, *et al*: Adiponectin and AdipoR1 regulate PGC-1alpha and mitochondria by Ca(2+) and AMPK/SIRT1. Nature 464: 1313-1319, 2010.
54. Yang B, Yang K, Chen J and Wu Y: Crocin protects the 661W murine photoreceptor cell line against the toxic effects of all-trans-retinal. Int J Mol Sci 25: 10124, 2024.
55. Mohammad Soleymani S, Assarzadegan F, Habibi SAH, Mahboubi A and Esmaily H: The effect of crocin on movement disorders and oxidative DNA damage in Parkinson's disease: Insights from a randomized controlled trial. Parkinsonism Relat Disord 126: 107051, 2024.